

Full-field particle velocimetry with a photorefractive optical novelty filter

Mike Woerdemann,^{a)} Frank Holtmann, and Cornelia Denz

Institut für Angewandte Physik, Westfälische Wilhelms-Universität, Corrensstraße 2/4, 48149 Münster, Germany

(Received 29 May 2008; accepted 11 June 2008; published online 15 July 2008)

We utilize the finite time constant of a photorefractive optical novelty filter microscope to access full-field velocity information of fluid flows on microscopic scales. In contrast to conventional methods such as particle image velocimetry and particle tracking velocimetry, not only image acquisition of the tracer particle field but also evaluation of tracer particle velocities is done all-optically by the novelty filter. We investigate the velocity dependent parameters of two-beam coupling based optical novelty filters and demonstrate calibration and application of a photorefractive velocimetry system. Theoretical and practical limits to the range of accessible velocities are discussed. © 2008 American Institute of Physics. [DOI: 10.1063/1.2955842]

A feasible method for experimental access to fluid flow velocities on microscopic scales is mandatory for understanding and improvement of microfluidic devices¹ as well as for many microbiological questions. Common velocimetry systems are micro particle image velocimetry² (μ PIV) and micro particle tracking velocimetry (μ PTV), which are adapted from their macroscopic analogs, PIV, and PTV.³ Seeding the fluid with tracer particles has proven to be a reliable concept but the subsequent digital evaluation as required for μ PIV/ μ PTV may show significant drawbacks, including the necessity for successive input images, time-consuming computations, or limitations of the underlying microscopy method.

In this letter, we propose an alternative approach to extract the velocity information of a seeding particle field. The presented method is based on all-optical image acquisition and preprocessing with a photorefractive novelty filter microscope⁴ and consequently will be called photorefractive velocimetry. We use a two-beam coupling based novelty filter,⁵ i.e., a two-dimensional (2D) implementation of photorefractive two-beam coupling.⁶ An image bearing signal beam is overlaid with a coherent reference beam within a photorefractive crystal. In steady state the novelty filter output equals zero intensity, due to the irreversible energy transfer from the signal beam to the reference beam. As a direct result of the interferometric nature of two-beam coupling, any novelty within the input signal instantaneously is detected as an intensity peak in the output signal. The novelty may be a change of amplitude or phase of any part of the input image.⁷ After detecting an input change, the output falls toward zero intensity within a characteristic time τ which is determined by the grating time constant τ_g of the photorefractive material.⁶ Although the decay of output intensity is known to be best described by an exponentially decaying term weighted by an infinite sum of Bessel functions,⁸ in most experimentally relevant situations it can be estimated very well by a purely exponential decay with an effective time constant τ .⁹

With this approximation, the output signal at time t is given by the difference of the current input and the integral over the time-exponential average of the input at all previous

times.¹⁰ Applying the temporal behavior of the optical novelty filter to each point of a 2D input image, the spatial behavior is obtained. Figure 1 shows the spatial intensity distribution for the simplest kind of object, a homogeneous square. In the filtered image the object exhibits trail formation, which is a characteristic feature of photorefractive novelty filters.⁹ While being undesired in some applications,^{7,11} it gives an easy access to the velocity of the underlying object.

Two characteristic parameters of a trail are its peak intensity I_{trail} and its length l_{trail} , i.e., the distance it takes for a decay down to $1/e$ of the peak intensity. A couple of important dependencies of these parameters are derived by a simple model. In this model a fixed point P within the trajectory of the object is chosen and movement of the object is discriminated into three periods. Initially the novelty filter input at P is background. Then, within a time span of $\Delta t = l/v$ the input equals the object amplitude and phase, followed by background again. Following this model, trail formation can be described by an exponential process, depending on Δt or its reciprocal $v_n = 1/\Delta t = v/l$, the normalized object velocity,

$$l_{\text{trail}} \propto v_n, \quad (1)$$

$$l_{\text{trail}} \propto \tau, \quad (2)$$

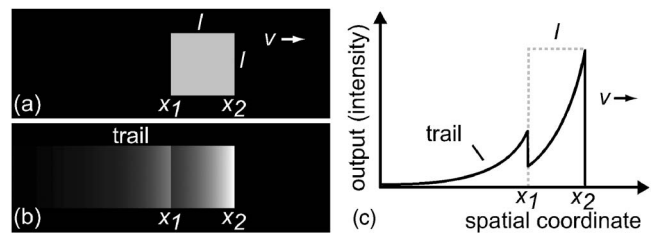


FIG. 1. Basic principle of trail formation. Original (a) and filtered image (b) of a square object of size l moving from left to right with velocity v . An intensity profile of the output is given in (c) as a solid line, whereas the input is indicated as an overlaid dotted line.

^{a)}Electronic mail: woerde@uni-muenster.de.

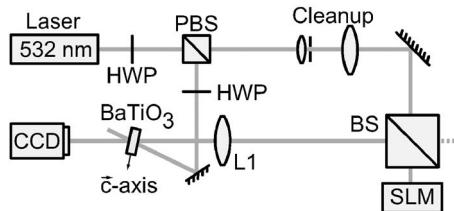


FIG. 2. Novelty filter setup using a SLM in reflection geometry. HWP, half wave plate; (P)BS, (polarizing) beam splitter; L1, imaging lens; cleanup, beam cleanup and expansion; laser, Nd:YAG emitting at 532 nm; CCD, video camera; BaTiO₃: photorefractive crystal.

$$I_{\text{trail}} \propto 1 - \exp\left(-\frac{1}{v_n \tau}\right). \quad (3)$$

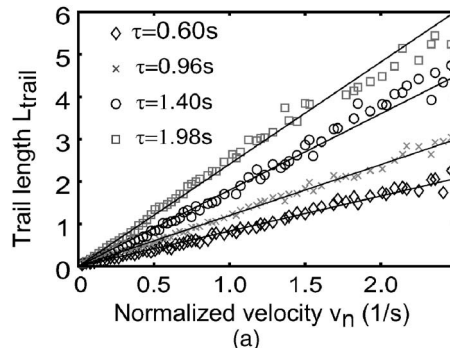
Validity of Eqs. (1)–(3) has been verified by a more sophisticated analysis, based on a detailed model¹² of photorefractive two-beam coupling, which derives from the photorefractive model of Kukhtarev *et al.*⁶ The linear relationship between the trail length and object velocity has also been shown experimentally by Mathey *et al.* for the special case of dark amplitude objects.¹³

The basic concept of photorefractive velocimetry is based on the unambiguous dependence of trail length and trail intensity on the object velocity. Trail length and object velocity correlate linearly [Eq. (1)] and thus enable measurement of the object velocity by simple determination of its trail length. Measurement of the trail intensity yields an additional, independent value for the object velocity and offers the opportunity of an instant validation of the measured velocity values. It is important to emphasize the instant accessibility of velocity information, in contrast to extensive computations as they are necessary in PIV/PTV correlation and tracking algorithms, respectively.

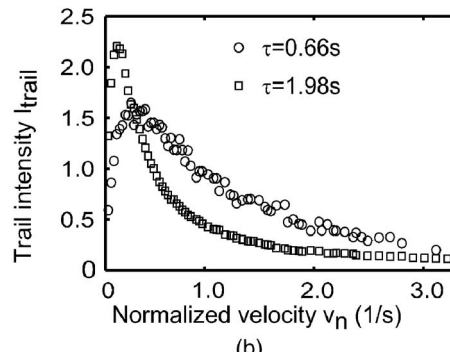
In order to proof the concept of photorefractive velocimetry, we implement a suitable novelty filter system. A spatial light modulator (SLM) is employed as the signal source and allows for maximum flexibility in the choice of objects and their velocities. This versatility is optimal for understanding trail formation and calibrating the system. We use a commercially available Hamamatsu phase modulator X8267-16 for phase modulation and a Holoeye LC 2002 for amplitude modulation. The Hamamatsu SLM operates in reflection geometry, while the Holoeye SLM requires transmission geometry.

As an example, Fig. 2 shows the experimental setup for the case of reflection geometry. A 45°-cut cerium-doped BaTiO₃ photorefractive crystal (5 × 4 × 3 mm³) is used to implement energy coupling between the signal bearing beam and a reference beam. The setup allows for adjusting the intensity ratio between the signal and the reference beam by tuning the first HWP. With additional neutral density filters, the total intensity on the crystal can be determined. In consequence, it is easy to adjust the system time constant in a wide range from approximately 0.5 to 10 s.

Detailed measurements of trail lengths and trail intensities for phase objects as well as dark and bright amplitude objects are performed. Figure 3(a) shows the dependence of the normalized trail length ($L_{\text{trail}} = l_{\text{trail}}/l$) on the normalized object velocity with the system time constant as a parameter, for the case of phase objects. There is a clear linear relationship as is suggested by Eq. (1). The slope is linearly related



(a)



(b)

FIG. 3. Dependence of trail length (top) and intensity (bottom) on particle velocity, measured for phase objects.

to the system time constant, in agreement with Eq. (2).

Measurements of the trail intensity for phase objects are shown in Fig. 3(b). An unambiguous relationship as expected by Eq. (3) can be shown for larger velocities. However, for smaller velocities $v \rightarrow 0$ a saturation is expected. The differing measurements in Fig. 3(b) can fully be explained by modulator effects which blur object edges and are not included in Eq. (3).

Corresponding measurements with the dark and bright amplitude objects yield equivalent results, except that the total trail intensity is lower. Even variation of the object phase φ does neither influence linearity nor slope of the dependence between trail length and particle velocity. Merely the intensity and thus detectability vary with the object phase, having a maximum at $\varphi = (2n+1)\pi$ and a minimum at $\varphi = 2n\pi$ and $n \in \{0, \pm 1, \pm 2, \dots\}$.

As a first example of application, we simulated a laminar tube flow on the SLM, taking dark amplitude objects as tracer particles. With the previously calibrated system, the particle velocities are detected by analyzing their trail lengths. Figure 4(b) faces the measured particle velocities with the known velocity distribution. As can be seen, the measured values differ less than 1 pixel/s from the expected ones.

Comparing photorefractive particle velocimetry with conventional (μ)PIV and (μ)PTV, one can see substantial similarities of both concepts. The task of measuring stream velocities is reduced to measuring tracer particle velocities in either case. Still there are significant differences in the actual process of determining particle velocities. While PIV/PTV fully relies on digital image processing, photorefractive velocimetry takes advantage of the all-optical image processing nature of optical novelty filters. As a consequence, full information of particle images—amplitude and phase information—can be used and thus there is no need for ad-

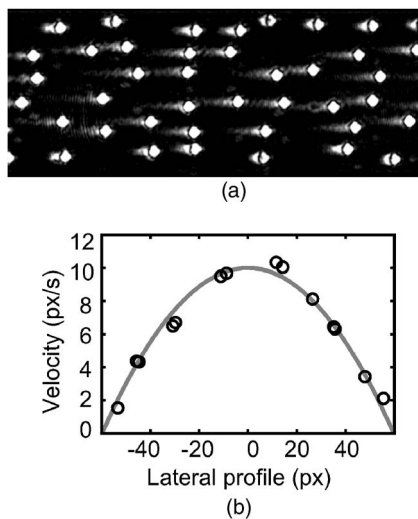


FIG. 4. Novelty filtered output of simulated particles tracing a laminar tube flow (top) and corresponding velocity profile (bottom). The parabolic curve shows the known velocity distribution and the dots indicate the velocities obtained by evaluating the trail lengths.

ditional marking or labeling specimen with all its possible drawbacks, especially in biological environments. Furthermore, in contrast to PIV/PTV, there is no need for a time series of images, but one single snapshot suffices to obtain full velocity information in the observation plane.

One of the most important figures of merit in velocimetry is the maximum measurable velocity. In our experiments, typically a maximum normalized velocity of $v_{n,\max} \approx 2.5$ is measured. Visibility of the trail is the limiting factor here. Taking Eq. (3) and introducing I_{\max} as the intensity that does not yet overexpose the camera and I_{\min} as the minimal required intensity for measuring the trail, one can get a good estimation for the maximum velocity as

$$v_{n,\max} = \frac{-1}{\tau \ln\left(1 - \frac{I_{\min}}{I_{\max}}\right)}. \quad (4)$$

If we evaluate this equation for typical experimental values $v_{n,\max} \approx 2.5$ and τ in the order of 1, a realistic value for the logarithmic term in Eq. (4) is received. Hence Eq. (4) reduces to

$$v_{n,\max} \approx 2.5/\tau, \quad (5)$$

showing the dependence of the maximum measurable velocity on the system time constant. The theoretical limit for the time constant of two-beam coupling with BaTiO_3 is about $\tau=0.002$ s.¹⁴ However, experimentally realized values are in the order of 0.1 s. On the other hand, time constants down to

0.005 s have been reached with polymeric photorefractive materials¹⁵ and hence should allow for normalized velocities up to $v_n \approx 500$. Current high-speed μPIV systems are able to resolve velocities of about 1000 $\mu\text{m/s}$.¹⁶ Assuming a comparable tracer particle diameter of 5 μm and an optimized photorefractive material, photorefractive velocimetry can be estimated to resolve velocities of the same order. A higher dynamic range of the camera system can be expected to extend the range of accessible velocities even more.

The lower limit of measurable velocity is given by the minimal detectable trail length. A typical value of the normalized velocity which could be measured is about $v_n=0.1$. With a tracer particle size of 5 μm , this would result in a minimal measurable velocity of 0.5 $\mu\text{m/s}$.

Summarizing our results, we have comprehensively investigated dependencies of all relevant parameters of trail formation on the velocity of objects. We could show an unambiguous dependence of trail length and trail intensity on the velocity of the underlying object over a wide range of velocity. In contrast to common full-field velocimetry techniques, photorefractive velocimetry does not require successive images, but enables extraction of full 2D velocity information out of one single snapshot. The choice of tracer particles is not limited to a specific kind, in particular, no fluorescence labeled particles are required. We demonstrated the suitability of photorefractive velocimetry experimentally in a first application and derived promising estimations for the possible range of accessible velocities.

- ¹G. M. Whitesides, *Nature (London)* **442**, 368 (2006).
- ²J. Santiago, S. Wereley, C. Meinhart, D. Beebe, and R. Adrian, *Exp. Fluids* **25**, 316 (1998).
- ³R. Adrian, *Exp. Fluids* **39**, 159 (2004).
- ⁴R. Cudney, R. Pierce, and J. Feinberg, *Nature (London)* **332**, 424 (1988).
- ⁵D. Anderson, D. M. Lininger, and J. Feinberg, *Opt. Lett.* **12**, 123 (1987).
- ⁶P. Yeh, *Introduction to Photorefractive Nonlinear Optics* (Wiley, New York, 1993).
- ⁷V. V. Krishnamachari and C. Denz, *J. Opt. A, Pure Appl. Opt.* **5**, 239 (2003).
- ⁸M. Horowitz, D. Kligler, and B. Fischer, *J. Opt. Soc. Am. B* **8**, 2204 (1991).
- ⁹M. Sedlatschek, T. Rauch, C. Denz, and T. Tschudi, *Opt. Commun.* **116**, 25 (1995).
- ¹⁰D. Anderson and J. Feinberg, *IEEE J. Quantum Electron.* **25**, 635 (1989).
- ¹¹V. Krishnamachari and C. Denz, *Appl. Phys. B: Lasers Opt.* **79**, 497 (2004).
- ¹²V. V. Krishnamachari, O. Grothe, H. Deitmar, and C. Denz, *Appl. Phys. Lett.* **87**, 071105 (2005).
- ¹³P. Mathey, B. Mazue, P. Jullien, and D. Rytz, *J. Opt. Soc. Am. B* **15**, 1353 (1998).
- ¹⁴P. Yeh, *Appl. Opt.* **26**, 602 (1987).
- ¹⁵O. Ostroverkhova and W. Moerner, *Chem. Rev. (Washington, D.C.)* **104**, 3267 (2004).
- ¹⁶Y. Sugii, R. Okuda, K. Okamoto, and H. Madarame, *Meas. Sci. Technol.* **16**, 1126 (2005).